Supplemental methods

Plasmids and transfection. Expression vectors for mouse wild-type SIRPα and its mutants lacking individual Ig-like domains (ΔV, ΔC1-1, ΔC1-2) were described previously (28). Full-length cDNAs for human SIRPα variant v1 (SIRPαv1), SIRPβ1, and SIRPγ were obtained from DNAFORM (Yokohama, Japan) and that for human SIRPβ2 was purchased from eurofins Genomics (Tokyo, Japan). A cDNA fragment encoding full-length human SIRPβ2 tagged with the Myc epitope at its COOH terminus (SIRPβ2myc) was generated by PCR with human *SIRPB2* cDNA as the template and an antisense primer containing the DNA sequence for the Myc epitope at its 5' end. To construct an expression vector for human SIRPαv1, SIRPβ1, SIRPβ2myc, and SIRPγ, we subcloned each full-length cDNA into the pcDNA3.1 vector (Thermo Fisher Scientific). An expression vector for mouse SIRPβ was described previously (29). A plasmid encoding human SIRPα variant v2 (SIRPαv2) protein were kindly provided by Nakayuki Honmma (Kyowa Hakko Kirin, Tokyo, Japan). For generation of expression vectors for MY-1 chimeric antibodies in which the constant region of MY-1 was replaced with that of mouse IgG2a, total RNA was purified from MY-1 hybridoma cells with the use of an RNeasy Mini Kit (Qiagen, Hilden, Germany). Complementary DNA fragments encoding the variable region of the heavy or light chain of MY-1 were amplified with the use of a 5'/3' RACE SMARTer RACE cDNA Amplification Kit (Takara, Kyoto, Japan) and Universal Primer Mix (Takara) and with either 5'-TGGTCTTTGGGGGGAAGATGAAGACAGATG-3' for the heavy chain or 5'-GACGGGGGAGGCTGATGTCTTATGAACAACCTCACAG-3' for the light chain. The resulting amplicons were further amplified by the polymerase chain reaction with the primers 5'-AAAAGAATTCACCATGGACATCAGGCTCAG-3' and 5'-TGAAGAGACAGTGACCAGAG-3' for the heavy chain or 5'-AAAAACCGGTGAGATGGAGACAGACAGACTC-3' and 5'-TTTGATCTCGAGCTTGGTCCC-3' for the light chain, and they were then

subcloned into pFUSE-CHIg (InvivoGen, San Diego, CA) for the heavy chain (yielding pFUSE-CHIg-MY-1) or into pFUSE2-CLIg (InvivoGen) for the light chain (yielding pFUSE2-CLIg-MY-1). HEK293A cells and FreeStyle 293-F cells were transfected with expression vectors with the use of Lipofectamine 2000 and 293Fectin (Thermo Fisher Scientific), respectively.

Preparation of MY-1 F(ab')$_2$ fragments. FreeStyle 293-F cells transiently transfected with pFUSE-CHIg-MY-1 together with pFUSE2-CLIg-MY-1 were cultured in FreeStyle 293 expression medium (Thermo Fisher Scientific) for 7 days. Chimeric MY-1 was then purified from the culture supernatant with the use of Protein G–Sepharose (GE Healthcare). The chimeric antibodies were cleaved with pepsin and subjected to gel filtration chromatography in order to purify the F(ab')$_2$ fragments.

Cell aggregation assay. A cell aggregation assay was performed as previously described (58), with slight modifications. For preparation of a single-cell suspension, cells were washed with PBS, incubated with 0.1% EDTA in PBS for 5 min at 37°C, and dispersed by gentle pipetting. The cells were then suspended at a density of 1×10^6/ml in Ca^{2+}- and Mg^{2+}-free HBSS supplemented with 10% FBS, DNase I (0.1 mg/ml), and 1 mM EDTA. For determination of the effects of mAbs to SIRPα, CHO-Ras cells stably expressing mouse SIRPα were incubated for 15 min at 37°C with MY-1, MY-1 F(ab')$_2$, P84, or normal rat IgG, each at a concentration of 5 μg/ml. Equal volumes of these cells and of CHO-Ras cells stably expressing mouse CD47 were then mixed together and incubated for 0 or 30 min at 37°C with gentle shaking. Formation of cell aggregates was terminated by the addition of glutaraldehyde to a final concentration of 2%, and the number of cells was counted with a hemocytometer. Aggregates of three or more cells were considered equivalent to single cells in this assay. The extent of cell aggregation

was then determined as the ratio of the number of cells at the end of the incubation (E_0 or E_{30} for 0 or 30 min) to that at its initiation (S).

Protein-based binding assay. The extracellular domain of mouse CD47 (aa 1–161) fused to human Fc (mouse CD47–Fc) was generated as described (58). The fusion proteins produced by cells cultured in serum-free DMEM/F-12 (1:1, v/v) medium was purified from the culture supernatants by chromatography on a column of protein A-Sepharose 4FF (GE Healthcare). A protein-based binding assay was performed as previously described (58), with slight modifications. In brief, confluence mouse SIRPα–expressing CHO-Ras (CHO-Ras-mSIRPα) cells as parental CHO-Ras cells in 96-well plate were washed twice with serum-free culture medium. The plates were then incubated with mouse CD47–Fc (10 μg/ml) of in the presence of MY-1 (100 μg/ml), P84 (100 μg/ml), or control rat IgG (100 μg/ml) in αMEM culture medium for 15 min at 37°C. The incubation medium for binding was aspirated and the wells were washed three times with ice-cold PBS. Cells were further incubated with HRP-conjugated goat pAbs specific to Fcγ fragment of human IgG (Jackson ImmunoResearch Laboratories) at 1:2000 dilution in PBS containing 1% BSA for 30 min at 4°C. Cells were then washed three times with PBS, and mouse CD47–Fc binding was determined by peroxidase activity using *o*-phenylenediamine dihydrochloride (Sigma-Aldrich) as a substrate. Absorbance at 450 nm of each wells was measured on a microplate reader (2030 ARVO X4, PerkinElmer).

Cell viability assay. For determination of cell viability, sodium 3'-[1-(phenylamino)-carbonyl]-3,4-tetrazolium]-bis(4-methoxy-6-nitro) benzenesulfonic acid hydrate (XTT) assay (Roche) was performed according to the manufacturer's protocol. Briefly, RENCA cells (1.0×10^4 cells/well) were seeded in 96-well plate and allowed to adhere overnight. Cells were further cultured in the presence or absence of

control IgG (10 μg/ml) or MY-1 (10 μg/ml) for 24 or 48 h. The cells were then incubated with the XTT labeling mixture for 4 h. The absorbance at 450 nm was quantitated by a microplate reader (2030 ARVO X4).

NK cell-mediated cytotoxicity assay. Assay of NK cell-mediated cytotoxicity was performed with the use of DELFIA europium (Eu) 2,2':6',2''-terpyridine-6,6''-dicarboxylic acid (TDA) cytotoxicity assay reagents (PerkinElmer, Waltham, MA) as previously described (12), with minor modifications. NK cells (effector cells) were isolated from the spleen of 8-week-old female BALB/c mice with the use of an NK Cell Isolation Kit II (Miltenyi Biotec, Cologne, Germany) and were cultured for 2 or 3 days in RPMI 1640 supplemented with 10% FBS, human recombinant IL-2 (1000 U/ml, PeproTech), and 50 μM 2-ME. The purity of the cells as analyzed by flow cytometry was >80%. RENCA cells (target cells) were labeled with TDA, washed, suspended in culture medium, plated in 96-well round-bottom plates (1×10^4 cells per well), and incubated for 4 h with various numbers of NK cells in the presence of antibodies (each at 5 μg/ml). The plates were then centrifuged, and 20 μl of each supernatant were transferred to the wells of a 96-well microtiter plate containing 200 μl of DELFIA Eu solution. The Eu forms a stable complex with TDA released into the medium from lysed target cells and generates fluorescence, which was measured with a time-resolved fluorometer (2030 ARVO X4). The percentage target cell lysis was calculated as: 100 × (experimental release – spontaneous release)/(maximal release – spontaneous release). Maximal release was determined by lysis of target cells with DELFIA lysis buffer; spontaneous release was measured by incubation of target cells in the absence of effector cells.

Table S1. Hematologic and blood biochemical analyses for C57BL/6 mice subjected intraperitoneal injection by MY-1, control IgG, or vehicle (-) three times a week for 2 weeks

Antibody	WBC ($\times 10^2$ cells /μl)	RBC ($\times 10^4$ cells /μl)	HGB (g/dl)	HCT (%)	PLT ($\times 10^4$ cells μl)
(-)	21.8±2.8	1003±24.5	15.0±0.3	47.2±1.4	81.5±20.3
IgG	22.7±5.1	996.8±21.0	14.9±0.6	48.2±0.9	71.3±16.7
MY-1	15.6±6.0	970.6±12.7	14.7±0.3	46.7±1.6	84.6±11.8

Antibody	Lymp (%)	Mono (%)	Neut (%)	Eos (%)	Baso (%)	Retic (%)
(-)	70.8±10.0	1.2±0.3	17.7±8.1	9.3±6.4	0.8±0.2	2.6±0.2
IgG	69.5±3.1	1.1±0.2	9.6±2.7	19±2.5	0.8±0.3	2.5±0.3
MY-1	66.1±11.3	0.7±0.2	11.3±3.5	21.1±12.5	0.7±0.3	4.0±0.8*

Antibody	Glc (mg/dl)	AST (U/l)	ALT (U/l)	ALP (U/l)	Total bilirubin (mg/dl)
(-)	178.8±35.1	40.8±3.6	15.6±1.5	698.8±77.5	0.11±0.22
IgG	178.3±23.4	39.0±1.8	14.0±1.2	701.5±44.0	0.10±0.01
MY-1	211.8±23.6	38.8±1.9	15.6±1.2	744.6±65.2	0.10±0.02

Antibody	BUN (mg/dl)	Total cholesterol (mg/dl)	Creatinine (mg/dl)	ALB (mg/dl)
(-)	17.7±2.70	54.0±3.2	0.12±0.02	3.61±0.14
IgG	17.6±1.11	63.0±5.1	0.10±0.01	3.39±0.04
MY-1	21.7±2.31	61.2±5.6*	0.12±0.01*	3.48±0.09

WBC, white blood cell; RBC, red blood cell; HGB, hemoglobin; HCT, hematocrit; PLT, platelet; Lymp, lymphocyte; Mono, monocyte; Neut, neutrophil; Eos, eosinophil; Baso, basophil; Retic, reticulocyte. Glc, glucose; AST, aspartate aminotransferase; ALT, alanine aminotransferase; ALP, alkaline phosphatase; BUN, blood urea nitrogen; ALB, albumin.

Data are means ± SEM for $n = 5$ mice per group. *$P < 0.05$ versus control IgG (one-way ANOVA and Tukey's test).

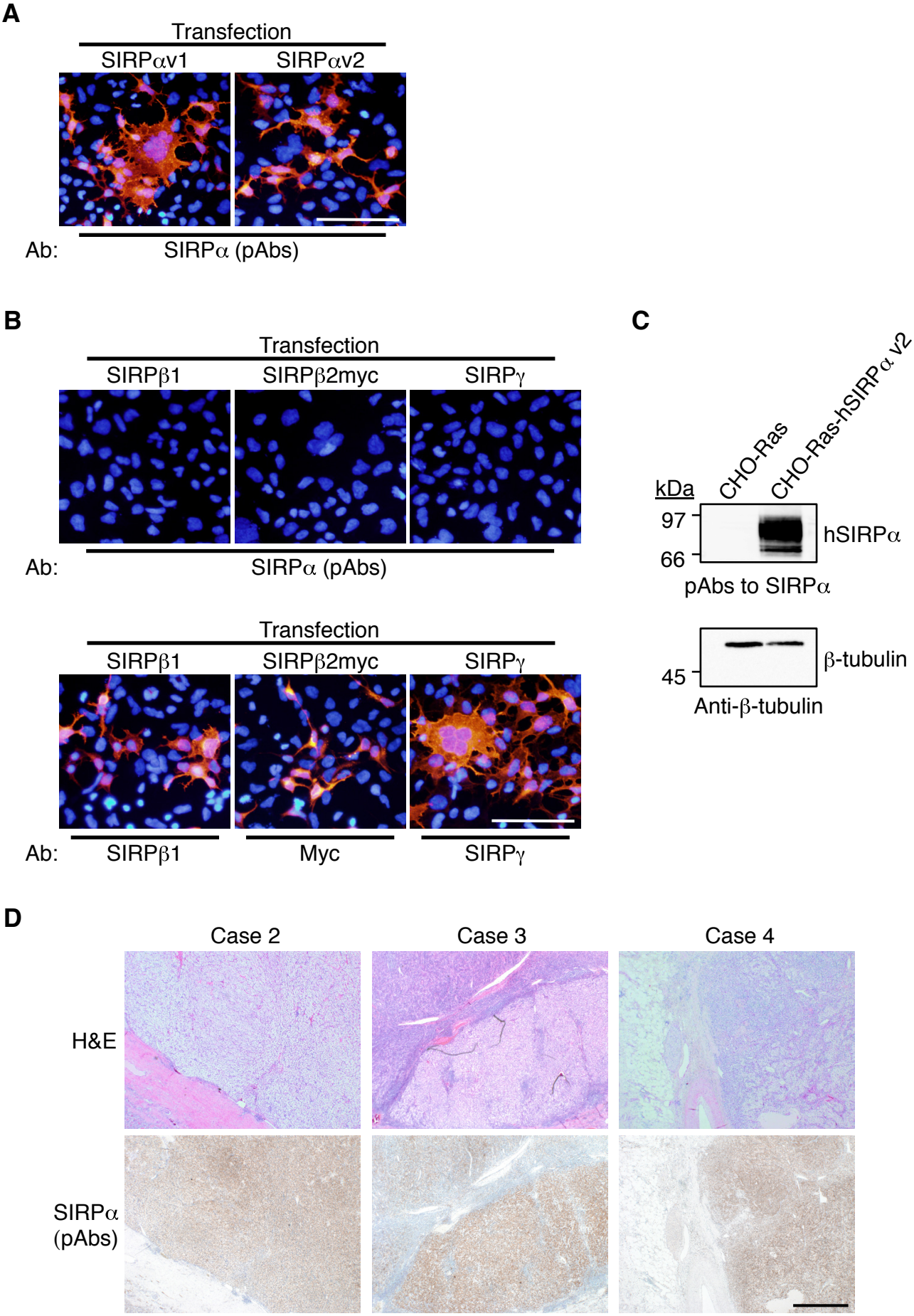

Supplemental Figure 1. Specificity of polyclonal antibodies (pAbs) to human SIRPα and expression of SIRPα in tumor tissue of patients with renal cell carcinoma. (**A** and **B**) HEK293A cells were transfected for 24 h with an expression vector for the indicated proteins, after which cells were fixed and subjected to immunofluorescence staining with pAbs to human SIRPα, or mAbs to human SIRPβ1, to Myc epitope tag (9E10), or to human SIRPγ as well as staining of nuclei with DAPI (blue). Rabbit pAbs to human SIRPα reacted with human SIRPα but not other human SIRP family members overexpressed in HEK293A cells. Scale bars, 100 μm. Images are representative of three separate experiments. (**C**) CHO cells stably expressing an active form of H-RAS either alone (CHO-Ras cells) or together with human SIRPα (CHO-Ras-hSIRPα cells) were subjected to immunoblot analysis with pAbs to human SIRPα and a mAb to β-tubulin (loading control). Data are representative of three separate experiments. (**D**) Paraffin-embedded tumor sections from patients with clear cell renal cell carcinoma (cases 2–4) were subjected to H&E staining as well as to immunohistochemical staining with pAbs to human SIRPα (brown) and to counterstaining with hematoxylin. Scale bar, 500 μm.

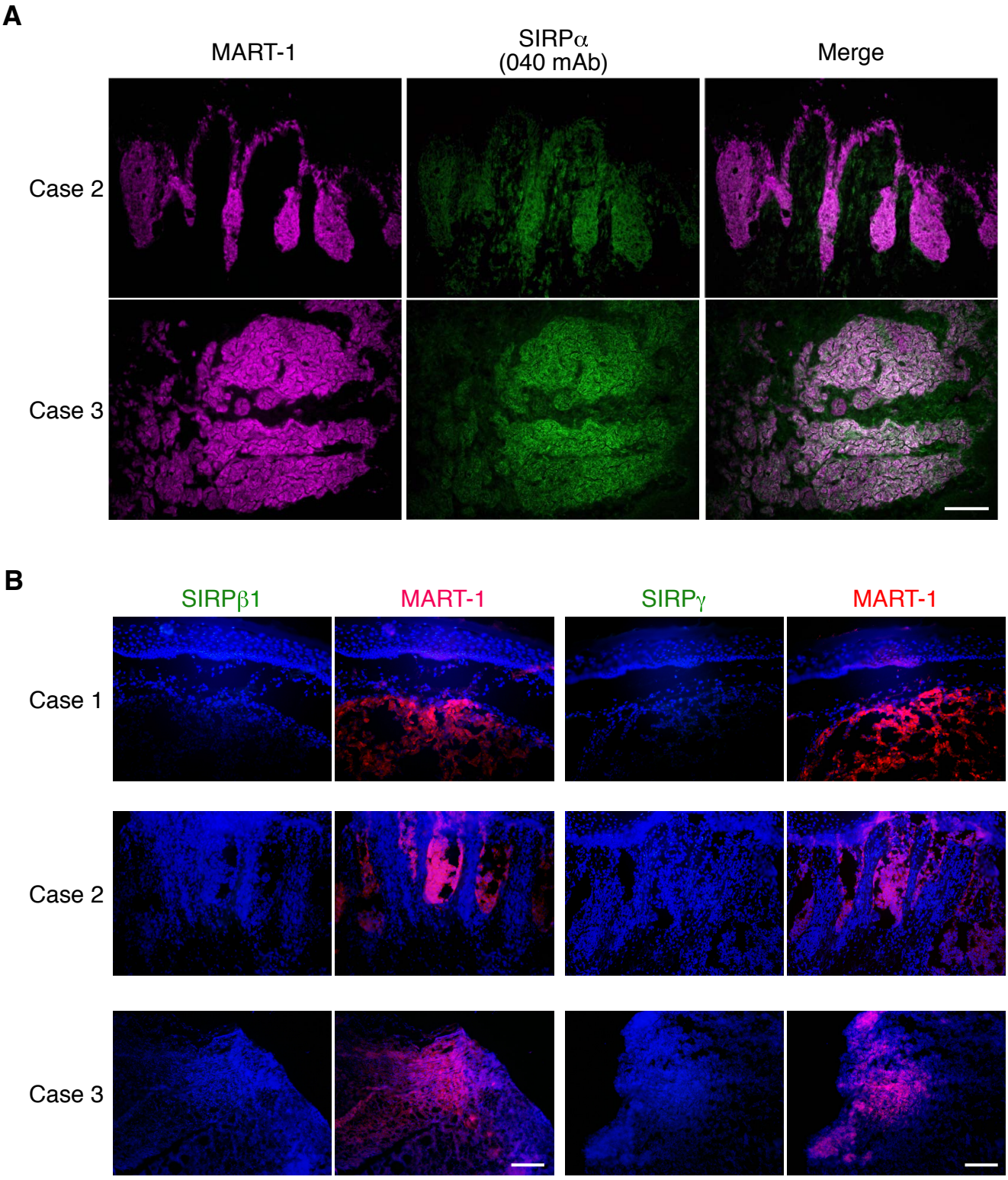

Supplemental Figure 2. Expression of SIRPα in tumor tissue of patients with melanoma. (**A**) Fresh frozen tumor sections of melanoma patients (cases 2 and 3) were subjected to immunofluorescence staining with mAbs to MART-1 (magenta) and to human SIRPα (040) (green). Scale bar, 100 μm. (**B**) Fresh frozen tumor sections of melanoma patients (cases 1–3) were subjected to immunofluorescence staining with a mAb to MART-1 (red) and either mAbs to human SIRPβ1 or to human SIRPγ (green) as well as staining of nuclei with DAPI (blue). Scale bars, 100 μm.

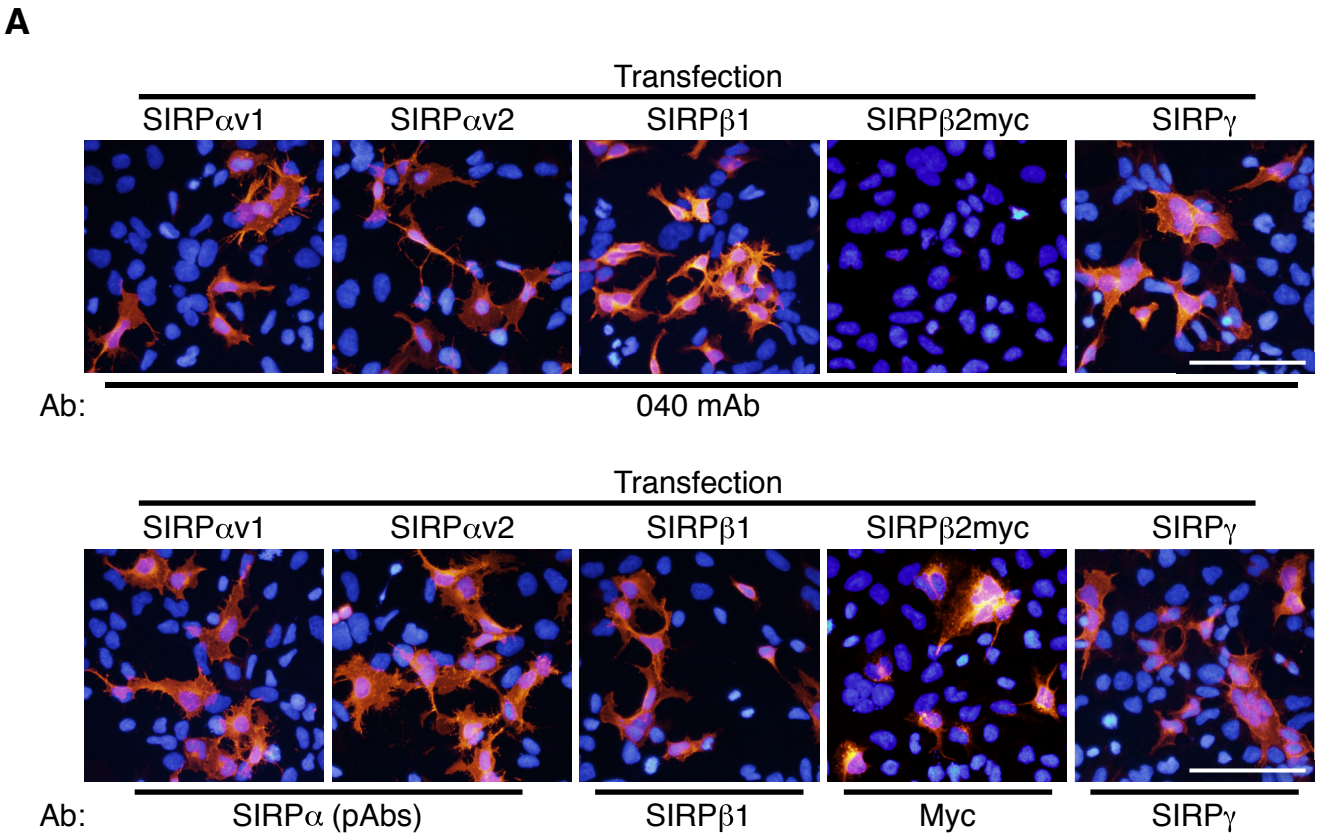

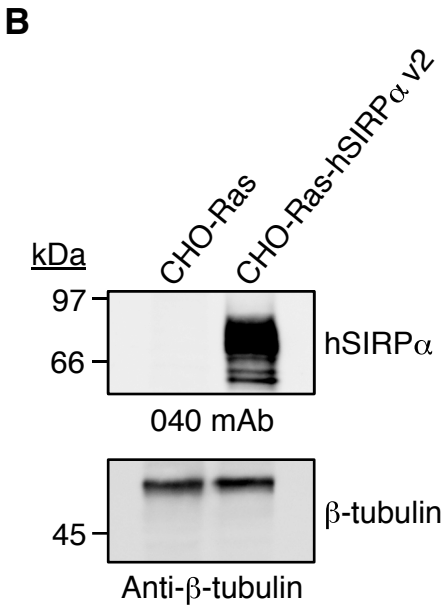

Supplemental Figure 3. Characterization of the 040 mAb. (**A**) HEK293A cells were transfected for 24 h with an expression vector for the indicated proteins, after which cells were fixed and subjected to immunofluorescence staining with the 040 mAb, polyclonal antibodies (pAbs) to human SIRPα, or mAbs to human SIRPβ1, to Myc epitope tag (9E10), or to human SIRPγ as well as staining of nuclei with DAPI (blue). The 040 mAb reacted with human SIRPα as well as human SIRPβ1 or SIRPγ overexpressed in HEK293A cells. Scale bars, 100 μm. Images are representative of three separate experiments. (**B**) CHO cells stably expressing an active form of H-RAS either alone (CHO-Ras cells) or together with human SIRPα (CHO-Ras-hSIRPα cells) were subjected to immunoblot analysis with the 040 mAb and a mAb to β-tubulin (loading control). Data are representative of three separate experiments.

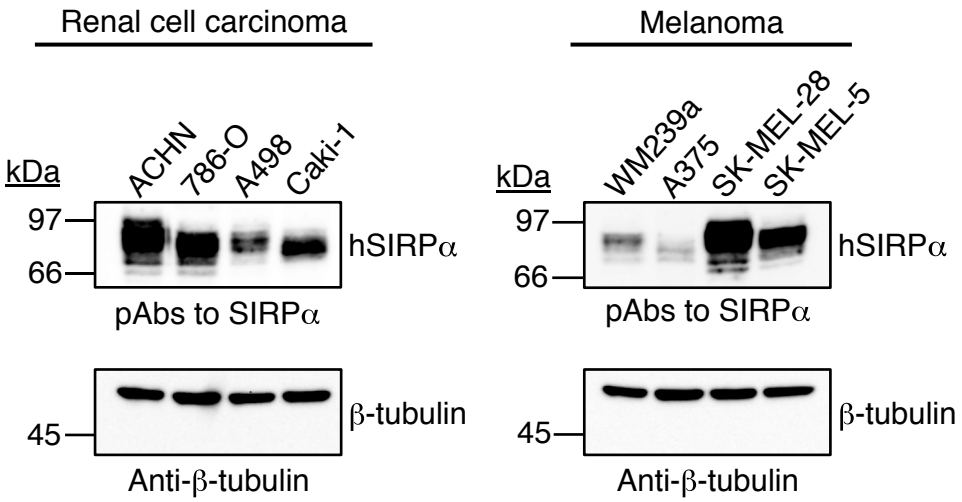

Supplemental Figure 4. Expression of SIRPα in human renal cell carcinoma and melanoma cell lines. Whole lysates of the indicated human renal cell carcinoma and melanoma cell lines were subjected to immunoblot analysis with polyclonal antibodies (pAbs) to human SIRPα and a mAb to β-tubulin. Data are representative of three separate experiments.

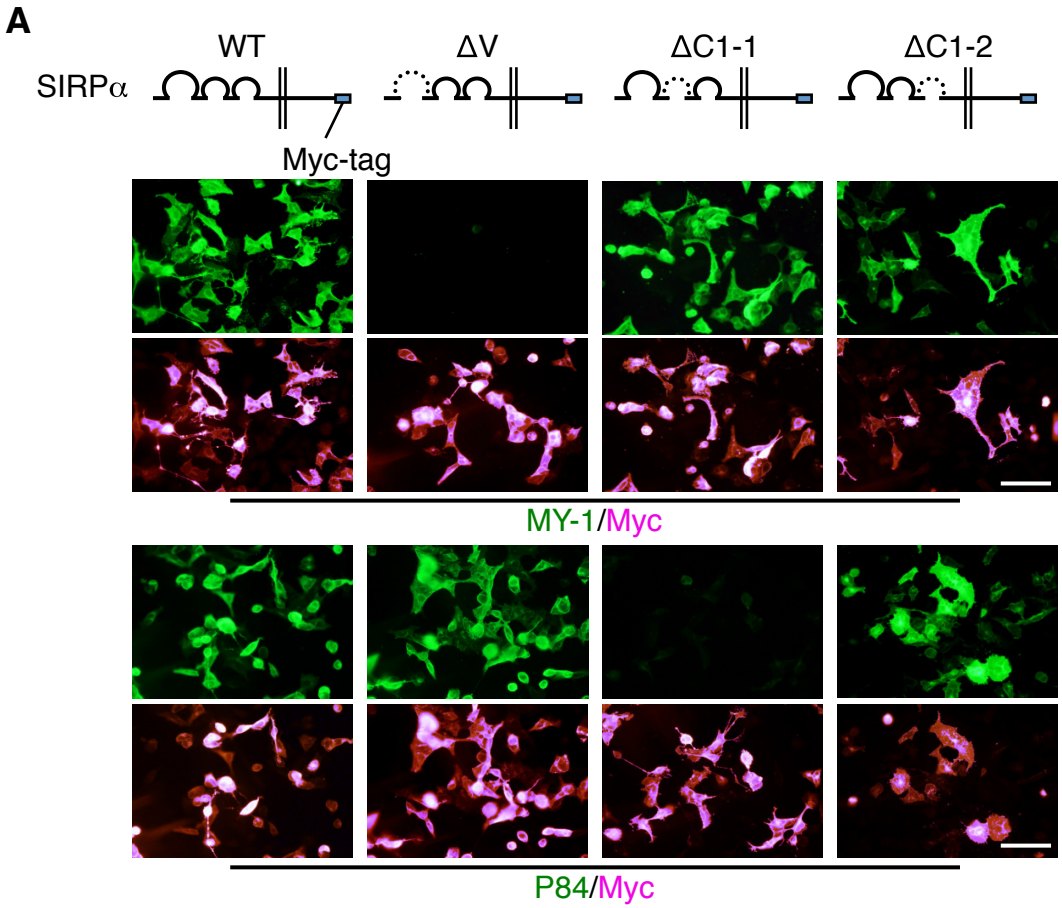

Supplemental Figure 5. Reactivity of MY-1 or P84 to mouse SIRP family members. (**A**) HEK293A cells were transfected for 24 h with an expression vector for wild-type (WT) or the indicated mutant (ΔV, ΔC1-1, ΔC1-2) forms of mouse SIRPα fused with a COOH-terminal Myc epitope tag. The cells were then fixed and subjected to immunofluorescence staining with mAbs to mouse SIRPα (MY-1 or P84) and to the Myc epitope tag (9E10). Immunoreactivity for MY-1 was not detected in cells expressing SIRPα(ΔV), whereas that for P84 was largely absent from those expressing SIRPα(ΔC1-1). Scale bars, 100 μm. (**B**) HEK293A cells were transfected for 24 h with an empty vector (-) or with an expression vector for mouse SIRPα or SIRPβ. The cells were then fixed and subjected to immunofluorescence staining with MY-1 or P84. Immunostaining revealed that MY-1 reacted with mouse SIRPα or SIRPβ overexpressed in HEK293A cells, whereas P84 did only with mouse SIRPα. Scale bar, 100 μm. All images are representative of three separate experiments.

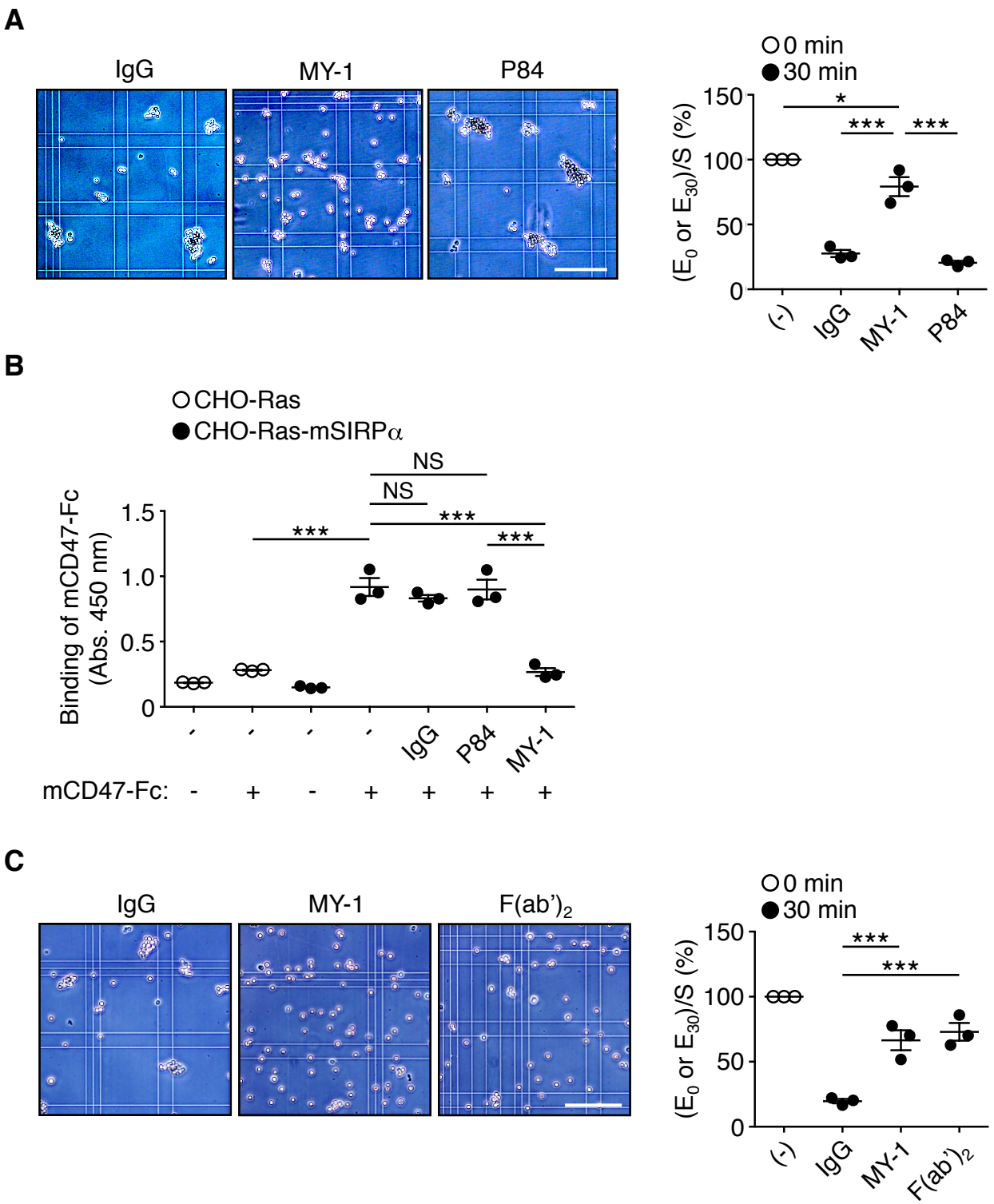

Supplemental Figure 6. Inhibition of the CD47-SIRPα interaction by MY-1 or F(ab')$_2$ fragments of MY-1 in vitro. (**A**) CHO-Ras cells stably expressing mouse SIRPα that had been exposed to mAbs to mouse SIRPα (MY-1 or P84), control IgG (IgG), or vehicle (–) were mixed and incubated for 0 or 30 min with CHO-Ras cells stably expressing mouse CD47. Representative hemocytometer images acquired after incubation for 30 min are shown in the left panel. Scale bar, 200 μm. Formation of aggregates by the two cell types was markedly inhibited by the prior treatment with MY-1. The extent of cell aggregation was also determined as the ratio of the number of separate cells or cell clusters at the end of the incubation (E_0, 0 min; E_{30}, 30 min) to that at its initiation (S) expressed as a percentage (right panel). (**B**) The binding of mouse CD47-Fc (mCD47-Fc) to either CHO-Ras cells stably expressing mouse SIRPα (CHO-Ras-mSIRPα) or CHO-Ras cells was determined in the presence or absence of MY-1, P84 or control IgG as described in the Supplemental Methods. (**C**) CHO-Ras cells stably expressing mouse SIRPα that had been exposed to control IgG, intact MY-1, or F(ab')$_2$ fragments of MY-1 were mixed and incubated for 30 min with CHO-Ras cells stably expressing mouse CD47. Representative hemocytometer images are shown in the left panel. Scale bar, 200 μm. The extent of cell aggregation was determined as in (**A**) (right panel). Quantitative data are means ± SEM of triplicate determinations ($n = 3$) and are representative of three separate experiments (**A**-**C**). *$P < 0.05$, ***$P < 0.001$, NS (one-way ANOVA and Tukey's test). Images are representative of three separate experiments. Abs, Absorbance.

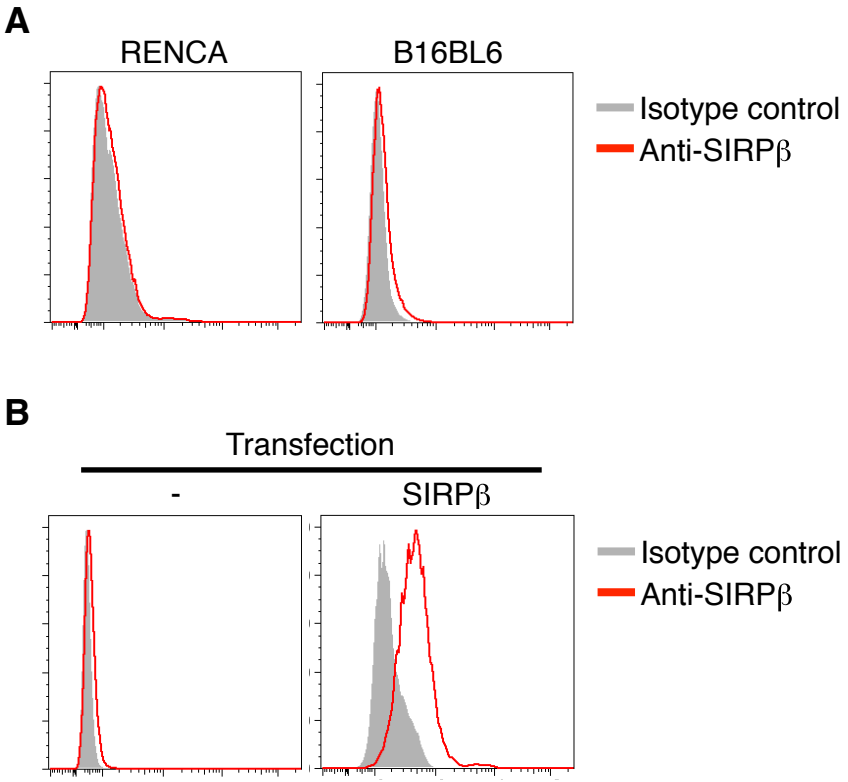

Supplemental Figure 7. Minimal expression of SIRPβ in RENCA and B16BL6 cells. (**A** and **B**) RENCA and B16BL6 cells (**A**) as well as HEK293A cells (**B**), which were transfected for 24 h with either an empty vector (-) or an expression vector for mouse SIRPβ, were incubated with a mAb to mouse SIRPβ (84) or an isotype control. The cells were then stained with propidium iodide and Alexa Fluor 488–conjugated polyclonal antibodies to rat IgG for determination of cell surface expression of SIRPβ by flow cytometry. Data are representative of three separate experiments.

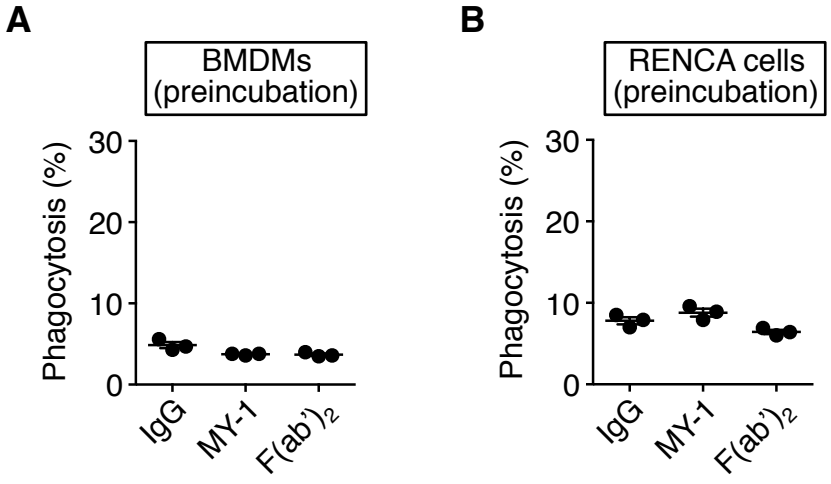

Supplemental Figure 8. Effect of preincubation of either bone marrow–derived macrophages (BMDMs) or CFSE-labeled RENCA cells with intact MY-1 or F(ab')$_2$ fragments of MY-1 on phagocytosis. (**A**) BMDMs from BALB/c mice were preincubated with intact MY-1 (10 μg/ml), F(ab')$_2$ fragments of MY-1 (10 μg/ml), or control IgG (IgG) (10 μg/ml) for 30 min, washed with PBS, mixed with CFSE-labeled RENCA cells, and further incubated for 4 h. Cells were then harvested, stained with a biotin-conjugated mAb to F4/80 and allophycocyanin-conjugated streptavidin as well as with propidium iodide, and analyzed by flow cytometry. The relative number of CFSE$^+$F4/80$^+$ BMDMs (BMDMs that had phagocytosed CFSE-labeled RENCA cells) is expressed as a percentage of all viable F4/80$^+$ cells. (**B**) CFSE-labeled RENCA cells were preincubated as in (**A**), washed with PBS, mixed with BMDMs from BALB/c mice, and further incubated for 4 h. Cells were then harvested, stained and analyzed as in (**A**). The relative number of CFSE$^+$F4/80$^+$ BMDMs is expressed as a percentage of all viable F4/80$^+$ cells. Data are means ± SEM of triplicate determinations (n = 3) and are representative of three separate experiments (**A** and **B**).

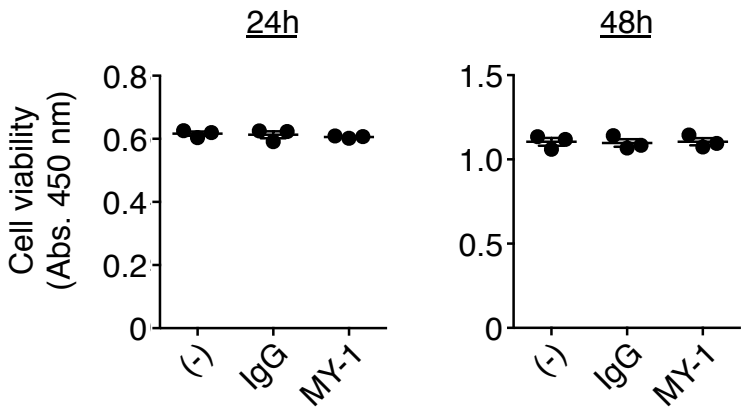

Supplemental Figure 9. Lack of effect of MY-1 on the viability of RENCA cells. RENCA cells were cultured for 24 or 48 h in the presence of MY-1 (10 μg/ml) or control IgG (IgG) (10 μg/ml). The cells were then incubated with the sodium 3'-[1-(phenylamino)-carbonyl]-3,4-tetrazolium]-bis(4-methoxy-6-nitro) benzenesulfonic acid hydrate (XTT) labeling mixture for 4 h. Cell viability was determined as the absorbance at 450 nm. Data are means ± SEM of triplicate determinations (n = 3) and are representative of two separate experiments. Abs, Absorbance.

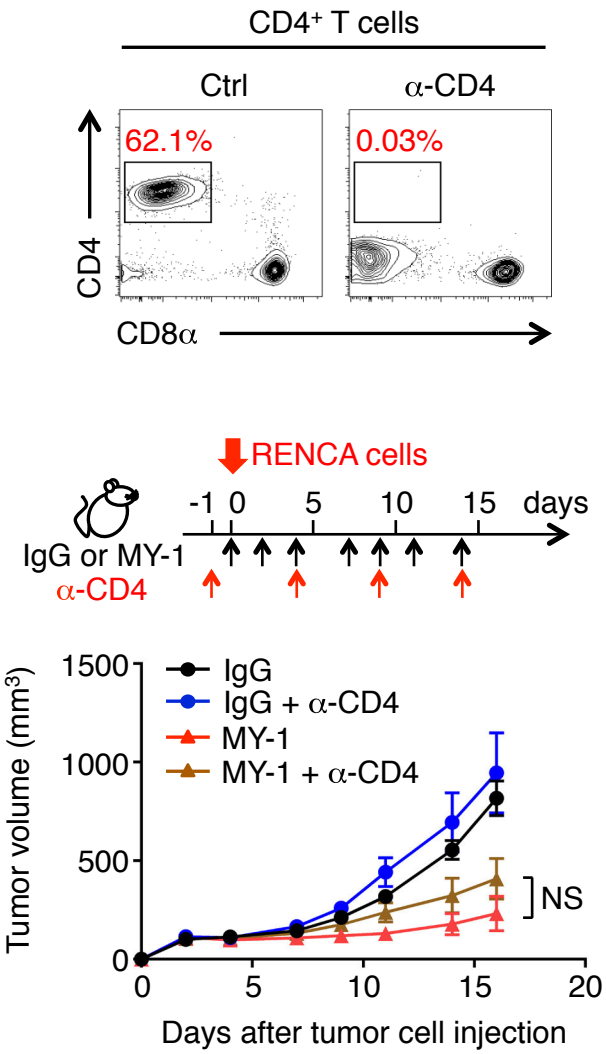

Supplemental Figure 10. Lack of effect of CD4⁺ T cell depletion on inhibition of RENCA tumor growth by MY-1. BALB/c mice were treated with either vehicle (Ctrl) or a mAb to CD4 (α-CD4), 4 days after which splenocytes were isolated from the mice, subjected to staining with a brilliant violet 510–conjugated mAb to CD45, an FITC-conjugated mAb to CD3ε, an allophycocyanin-conjugated mAb to CD4, and a phycoerythrin-conjugated mAb to CD8α as well as with propidium iodide, and analyzed by flow cytometry. The relative number of CD4⁺ T cells is expressed as a percentage of all viable CD45⁺CD3ε⁺ splenocytes on each plot (upper panel). BALB/c mice were also treated with either vehicle or a mAb to CD4 (α-CD4), injected with RENCA cells, and treated with MY-1 or control IgG (IgG) according to the indicated schedule for determination of tumor volume at the indicated times (lower panel). Data are representative of three separate experiments (upper panel) or are means ± SEM for *n* = 10 mice per group examined in two separate experiments (lower panel). NS (two-way ANOVA and Tukey's test).

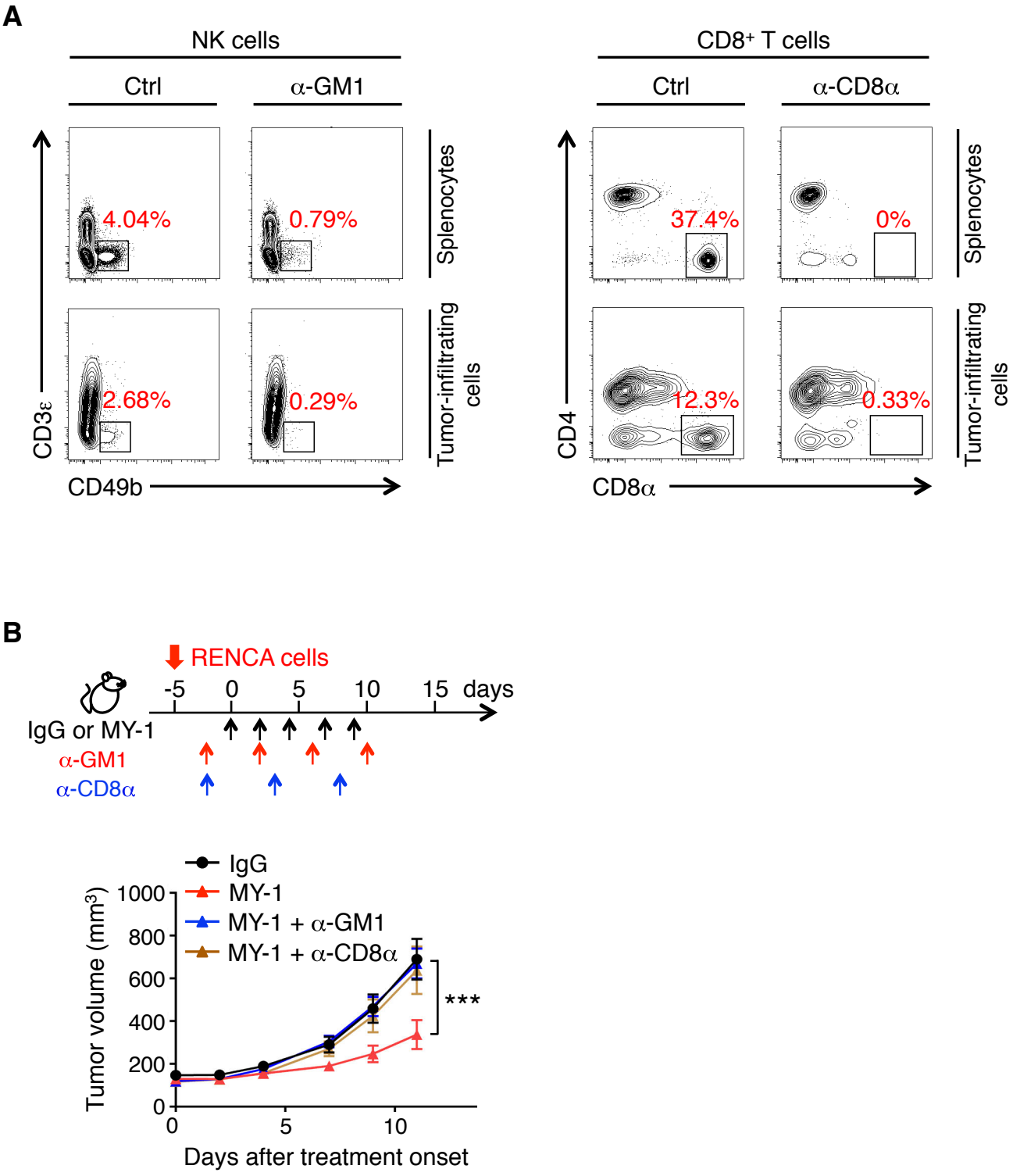

Supplemental Figure 11. Importance of NK cells and CD8⁺ T cells in inhibition of tumor growth by MY-1 in mice with established RENCA tumors. (**A**) BALB/c mice with established RENCA tumors (an average size of 100 to 150 mm^3) were injected with either vehicle (Ctrl), polyclonal antibodies (pAbs) to asialoganglioside GM1 (α-GM1), or a mAb to CD8α (α-CD8α), 3 days after which splenocytes or tumor-infiltrating cells were isolated from the mice, subjected to staining with propidium iodide and a brilliant violet 510–conjugated mAb to CD45 as well as with either a phycoerythrin (PE)–conjugated mAb to CD3ε and an FITC-conjugated mAb to CD49b (left panel) or an FITC-conjugated mAb to CD3ε, an allophycocyanin-conjugated mAb to CD4, and a PE-conjugated mAb to CD8α (right panel), and analyzed by flow cytometry. The relative numbers of NK cells (left panel) and CD8⁺ T cells (right panel) were expressed as a percentage of all viable CD45⁺ and CD45⁺CD3ε⁺ cells on each plot, respectively. (**B**) BALB/c mice were injected with pAbs to asialo-GM1 or a mAb to CD8α (α-CD8α), RENCA cells, and either MY-1 or control IgG (IgG) according to the indicated schedule. Tumor volume was measured at the indicated times. Data are representative of three separate experiments (A) or are means ± SEM for $n = 12$ (IgG), $n = 10$ (MY-1 or MY-1 + α-GM1), or $n = 9$ (MY-1 + α-CD8α) mice in two separate experiments (**B**). ***$P < 0.001$ (two-way ANOVA and Tukey's test).

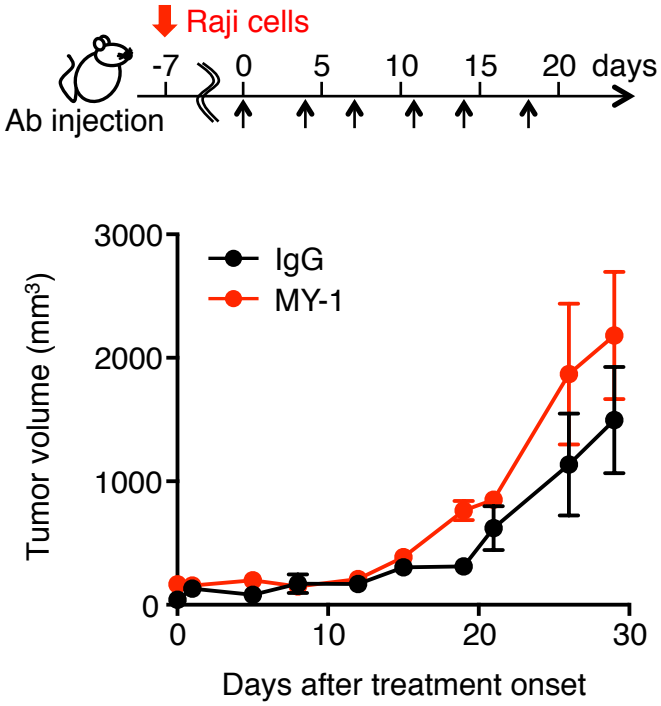

Supplemental Figure 12. Lack of effect of MY-1 on tumor formation by Raji cells in NOD/SCID mice. NOD/SCID mice were injected subcutaneously with Raji cells and treated with control IgG (IgG) or MY-1 twice a week beginning when the tumors became palpable (on day 7). Tumor volume was then measured every 2 to 3 days. Data are means ± SEM for $n = 3$ mice per group and are representative of two separate experiments.

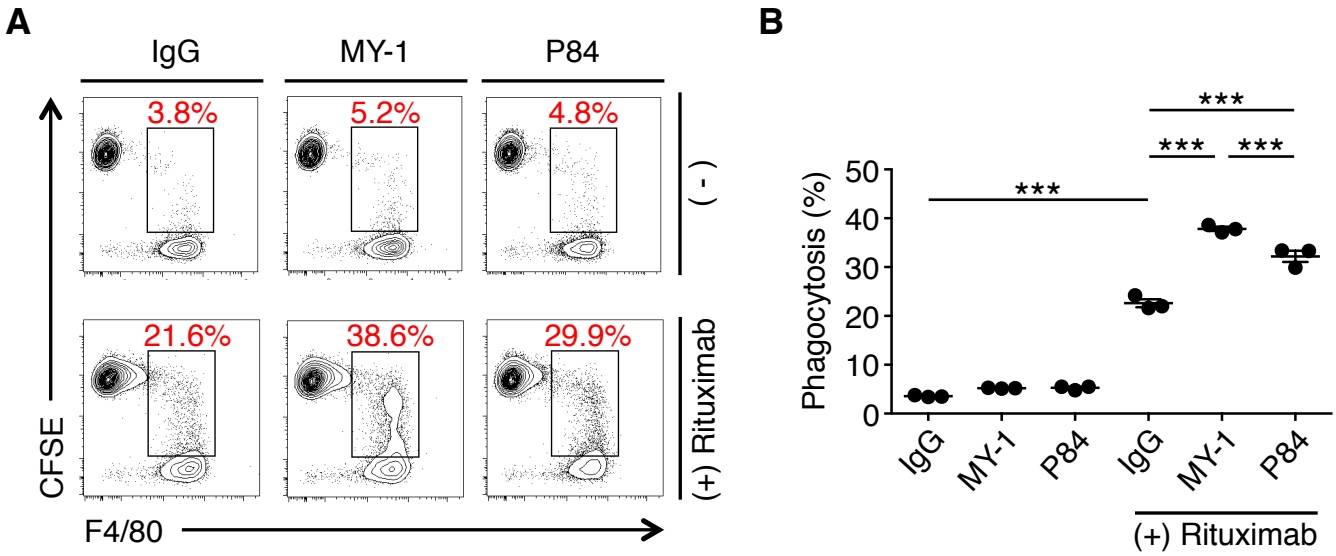

Supplemental Figure 13. Enhancement by antibodies to SIRPα of rituximab-induced phagocytosis of Raji cells by macrophages. (**A**) CFSE-labeled Raji cells were incubated for 4 h with bone-marrow derived macrophages (BMDMs) from NOD mice in the presence of control IgG (IgG) (10 μg/ml), MY-1 (10 μg/ml), P84 (10 μg/ml), control IgG plus rituximab (each at 5 μg/ml), MY-1 plus rituximab (each at 5 μg/ml), or P84 plus rituximab (each at 5 μg/ml). Cells were then harvested, stained with a biotin-conjugated mAb to F4/80 and allophycocyanin-conjugated streptavidin as well as with propidium iodide, and analyzed by flow cytometry. The relative number of $CFSE^+F4/80^+$ BMDMs is expressed as a percentage of all viable $F4/80^+$ cells on each plot. (**B**) The percentage of such $CFSE^+F4/80^+$ BMDMs among viable $F4/80^+$ cells was also determined. Data are representative of three separate experiments [(**A** and **B**); means ± SEM of triplicate determinations (n = 3) in (**B**)]. $^{***}P < 0.001$ (one-way ANOVA and Tukey's test).

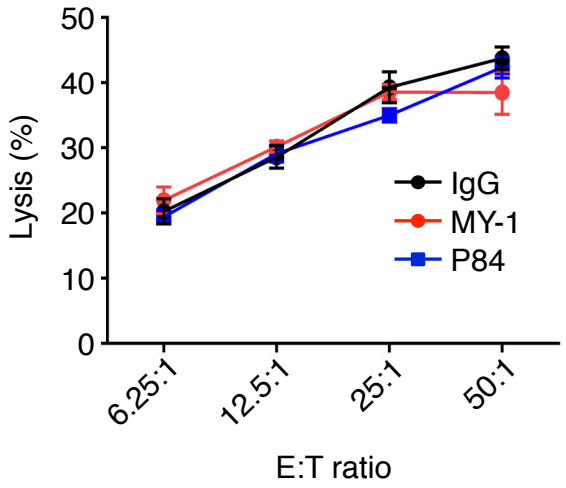

Supplemental Figure 14. Lack of effect of MY-1 or P84 on NK cell–mediated cytotoxicity toward RENCA cells. RENCA cells (target cells) were labeled with TDA (2,2':6',2''-terpyridine-6,6''-dicarboxylic acid) and incubated for 4 h with NK cells (effector cells) at the indicated E (effector):T (target) ratios in the presence of control IgG, MY-1, or P84. The extent of target cell lysis was then determined on the basis of the amount of TDA released into the medium. Data are means ± SEM of triplicate determinations ($n = 3$) from an individual experiment and are representative of three separate experiments.